SUPPORTING INFORMATION

Ultrafast Time Resolved Infrared Spcectroscopy Study on the Photochemistry of N,N-Diethyldiazoacetamide. Rearrangement in the Excited State (RIES)

Yunlong Zhang[a], *Gotard Burdzinski*[b], *Jacek Kubicki*[b], *and Matthew S. Platz*[a]*

[a] Department of Chemistry, The Ohio State University, 100 West 18th Avenue, Columbus, Ohio, 43210, U.S.A.

[b] Quantum Electronics Laboratory, Faculty of Physics, Adam Mickiewicz University, 85 Umultowska, Poznan 61-614, Poland

Table of Contents

Ultrafast IR pump-probe absorption measurements were performed using the home-built spectrometer at the Ohio State University. Solution concentrations were adjusted to absorption of unity in a 1 mm cell. Sample solutions were excited in a stainless steel flow cell equipped with 2 mm thick BaF_2 windows. After passing the sample reference and probe beam were spectrally dispersed with a polychromator and independently imaged on a liquid-nitrogen cooled HgCdTe detector (2 x 32 pixels). The pump pulse energy was about 4 μJ at the sample position. The entire set of pump-probe delay positions (cycle) is repeated at least three times, to observe data reproducibility from cycle to cycle. To avoid rotational diffusion effects, the angle between polarizations of the pump beam and the probe beam was set to the magic angle (54.7°). Kinetic traces are analyzed by fitting to a sum of exponential terms. All experiments were performed at room temperature.

Ground state geometry optimizations were carried out using Becke's three-parameter hybrid exchange functional with the Lee-Yang-Parr correlation functional (B3LYP)[1-4] as implemented in Gaussian 03[5]. In order to approximate the experimental condensed phase and to evaluate the effect of different solvents, the polarizable continuum model (PCM)[6] implemented in Gaussian 03 was utilized. Transition states were located with QST2 method implemented in Gaussain 03. Vibrational frequency analyses were performed to verify that the stationary points obtained corresponded to energy minima. The absolute energies of optimized structures are in Hartrees. All calculations were performed at The Ohio Supercomputer Center.

Figure S1. FTIR spectra of N,N-diethyl diazoacetamide in chloroform.

The diazoamide chloroform solution was bleached solution with 266 nm light for a few minutes and the UV-vis absorption at 270 nm decreased significantly. The FTIR spectra taken before and after bleach show the formation of β– lactam (1740 cm^{-1}) and γ-lactam (1670 cm^{-1}) upon photolysis. Similarly the diazoamide methanol-O-*d* solution was also bleached, and the bleached solution was evaporated to remove the solvent, dissolved in chloroform and the FTIR spectra (dashed red curve) show the formation of amide ether band at 1640 cm^{-1}, in addition to the β– and γ-lactams. Authentic sample of γ-lactam was purchased from Aldrich. The harmonic frequencies (scaled with 0.978) in chloroform calculated from the PCM model with B3LYP/6-31+G(d) level of theory for the C=O stretching in diazoamide, the β-and γ-lactams, and singlet carbene were also included for comparison.

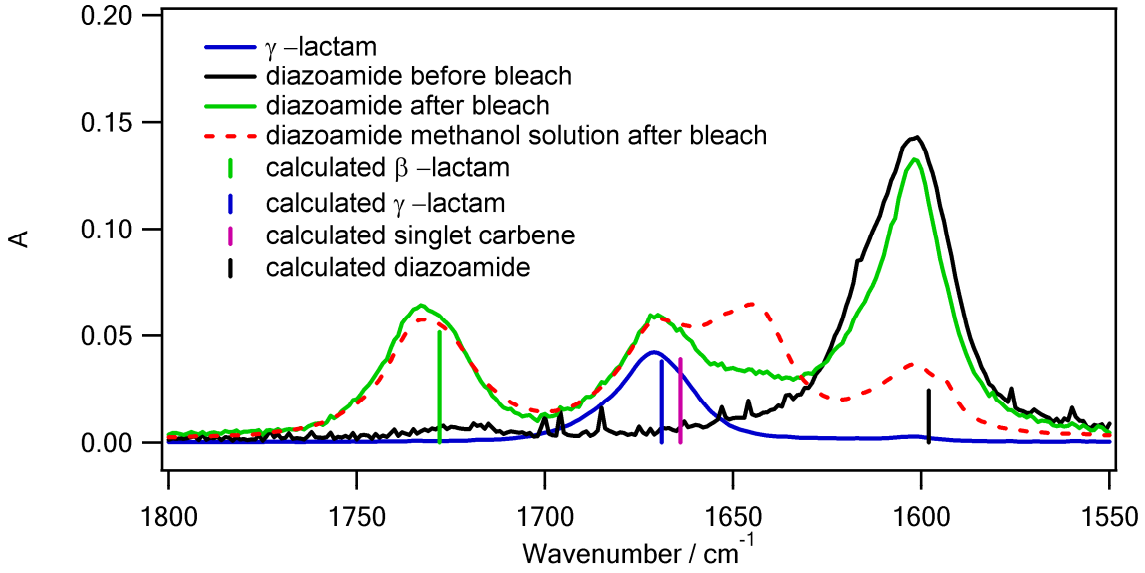

Figure S2. Ultrafast IR spectroscopy (270 nm) of N,N-diethyl diazoacetamide in chloroform. (a) The kinetic trace at 1745 cm^{-1} fitted into an exponential function. (b) The kinetic trace at 1669 cm^{-1} fitted into an exponential function.

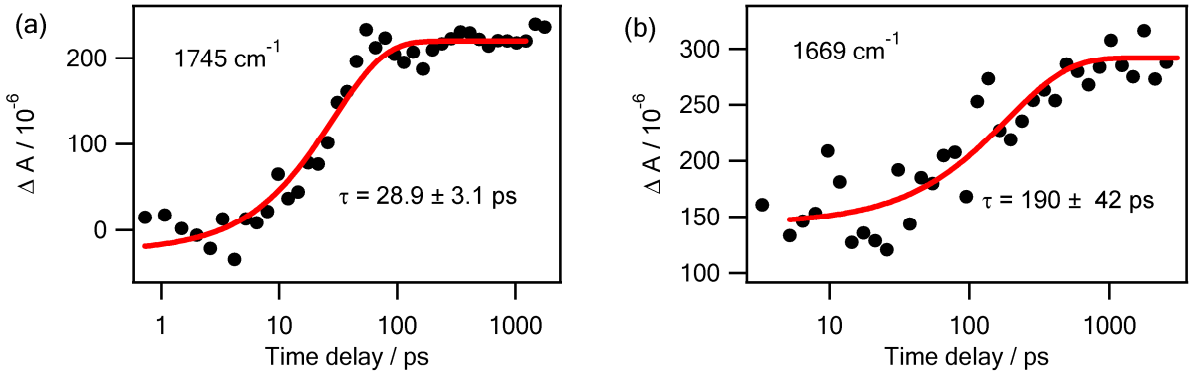

Figure S3. FTIR spectra of N,N-diethyl diazoacetamide in methanol-O-*d*.

The N,N-diethyl diazoacetamide solution in methanol-O-*d* was bleached with 266 nm light, and the FTIR spectra were taken before and after bleach. The authentic sample of γ-lactam was purchased from Aldrich. The authentic sample of amide ether was prepared from condensation of methoxyacetic chloride with diethylamine. The harmonic frequencies (scaled with 0.978) in methanol calculated from the PCM model with B3LYP/6-31+G(d) level of theory for the C=O stretching in diazoamide, the β-and γ-lactam, singlet carbene and amide ether were also included for comparison. The intensity of the predicted C=O stretching mode were scaled by $\times 10^{-4} - 10^{-5}$.

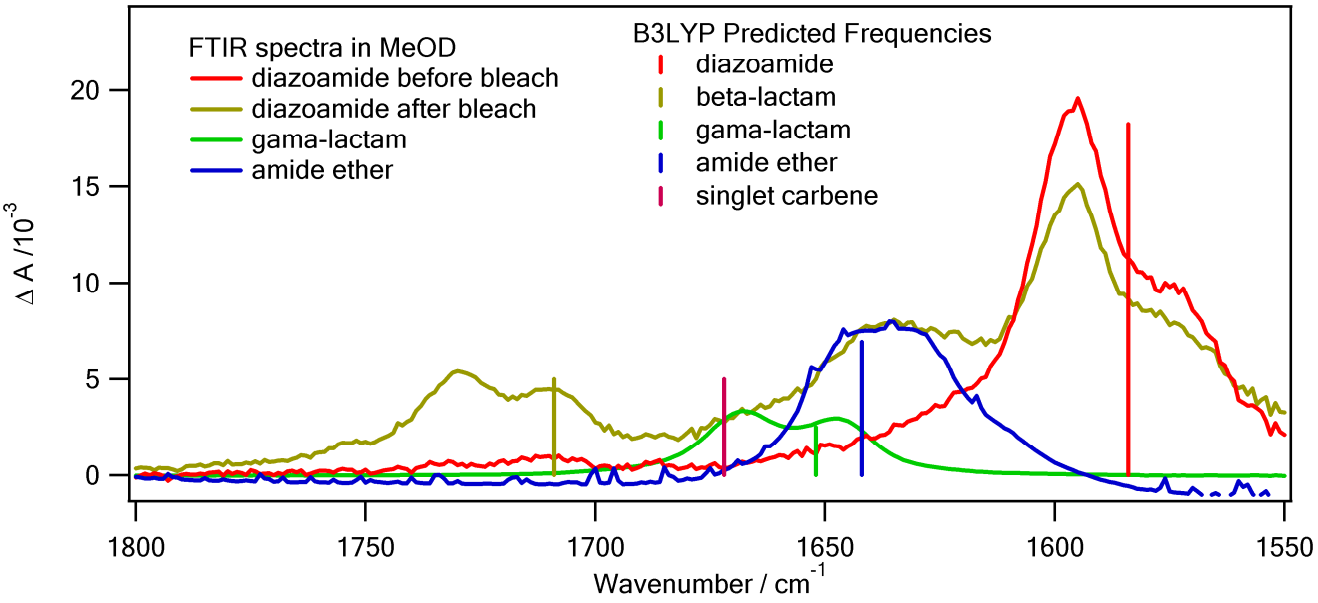

Figure S4. 2D contour plots from ultrafast IR spectroscopy (270 nm) of N,N-diethyl diazoacetamide in methanol-O-*d*.

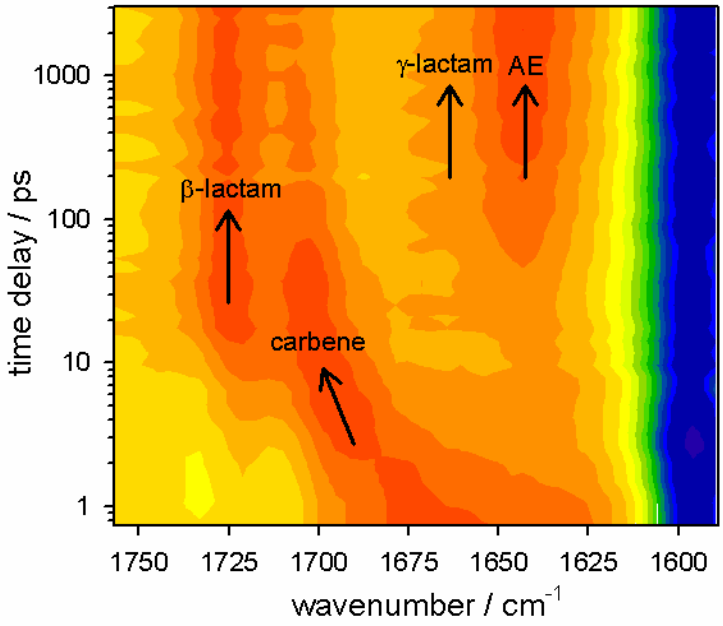

Figure S5. Ultrafast IR spectroscopy (270 nm) of N,N-diethyl diazoacetamide in methanol-O-*d*. (a) The kinetic trace at 1733 cm^{-1} fitted into an exponential function. (b) The kinetic trace at 1665 cm^{-1}.

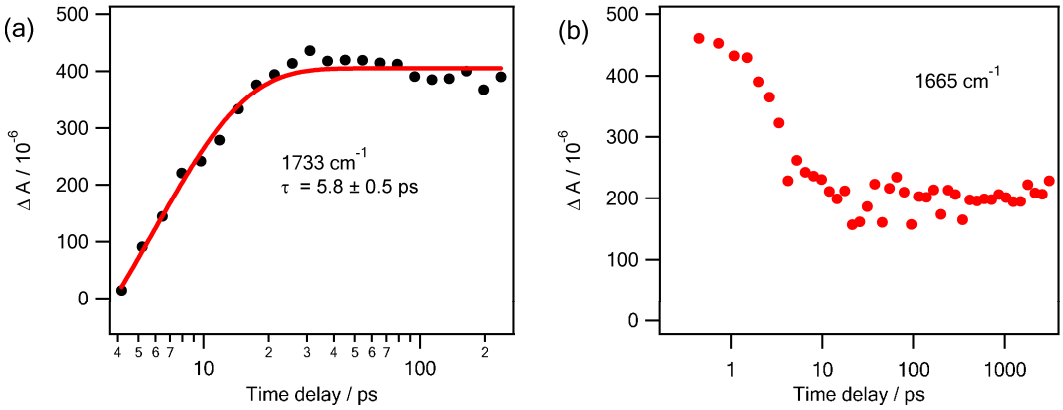

Figure S6. Ultrafast IR spectroscopy (270 nm) of N,N-diethyl diazoacetamide in methanol-O-*d*. (a) The kinetic trace at 1706 cm^{-1} fitted into an exponential function. (b) The kinetic trace at 1706 cm^{-1} fitted into an exponential function.

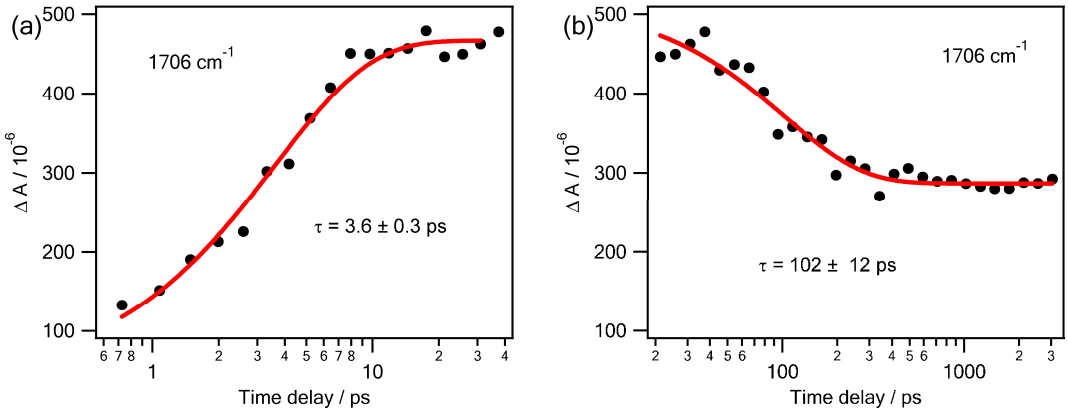

Figure S7. Ultrafast IR spectroscopy (270 nm) of N,N-diethyl diazoacetamide in methanol-O-d. The kinetic trace at 1643 cm^{-1} fitted into an exponential function.

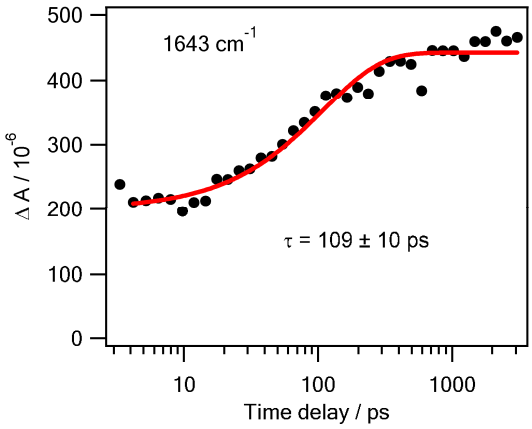

Figure S8. The transition states for the formation of γ-lactam (TS1) and β-lactam (TS2) calculated at the B3LYP/6-31+G(d) level of theory. Free energies (ΔG) are in kcal/mol at 298K in the gas phase. ZPE was corrected.

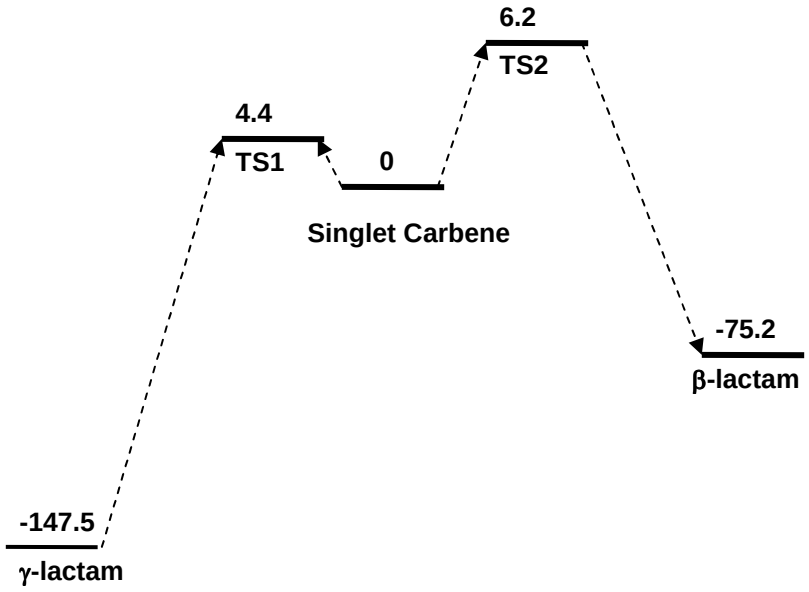

Table S1. The calculated frequencies (cm^{-1}) for the carbonyl stretching mode in singlet carbene, β-lactam, γ-lactam , amide ether, cation, and diazoamide in the gas phase, in chloroform and methanol with PCM model at the B3LYP/6-31+G(d) level of theory. Frequencies were not scaled.

Compound	Gas Phase (intensity)	Chloroform (intensity)	Methanol (intensity)
Carbene	1699 (532)	1707 (783)	1709 (892)
γ-lactam	1767 (452)	1712 (760)	1689 (919)
β-lactam	1832 (635)	1773 (1033)	1748 (1229)
amide ether	1719 (383)	1687 (605)	1679 (749)
cation	1911 (308)	1907 (446)	1906 (505)
diazoamide	1683 (293)	1639 (492)	1620 (606)

Table S2. Optimized structure of the transition state TS1 from singlet carbene to gama-lactam and B3LYP/6-31+G(d) level of theory. Transition state were obtained from QST2 method and were confirmed with IRC calculation.

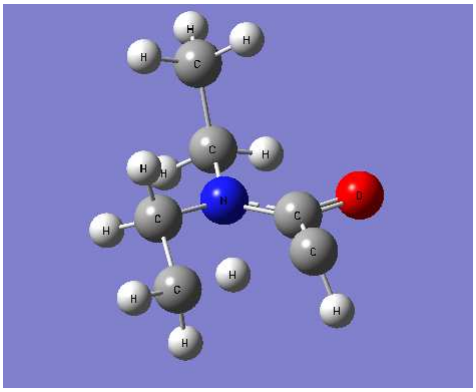

Energy = -365.12479850

C	0.46256	0.98237	-0.01857
C	1.78983	1.02794	0.56257
H	2.51525	1.4081	-0.17104
O	-0.02886	2.12431	-0.11908
N	-0.18383	-0.18356	-0.31392
C	0.46825	-1.4429	0.03378
H	0.20329	-1.75316	1.05643
H	0.10856	-2.22349	-0.64831
C	1.98148	-1.29482	-0.07683
H	2.51363	-2.15585	0.34245
H	2.32116	-1.10582	-1.09705
H	2.30731	-0.44333	0.62646
C	-1.61427	-0.1622	-0.62222
H	-1.79739	-0.90736	-1.40733
H	-1.82763	0.82502	-1.03958
C	-2.51594	-0.42529	0.58956
H	-2.34857	0.32882	1.36606
H	-3.56904	-0.37664	0.28772
H	-2.34042	-1.41653	1.02453

Frequency (cm^{-1})	IR intensity (km/mol)	Frequency (cm^{-1})	IR intensity (km/mol)	Frequency (cm^{-1})	IR intensity (km/mol)
-298	82.3	948	6.1	1502	35.0
60	2.6	964	24.3	1517	13.8
111	2.2	1021	31.1	1523	2.8
171	0.3	1060	22.5	1542	27.3
183	1.8	1099	9.1	1558	6.5
219	1.3	1110	4.8	1632	311.2
324	13.7	1159	15.1	2333	148.8
358	5.5	1207	7.6	3010	44.6
390	15.5	1261	13.3	3047	30.9
479	11.3	1300	3.9	3048	39.2
513	0.5	1342	118.7	3064	26.7
596	19.9	1368	6.1	3086	8.3
632	23.5	1401	22.0	3092	20.7
702	3.8	1407	10.3	3105	22.1
794	3.9	1432	11.9	3123	23.5
830	0.9	1468	1.6	3136	13.6
882	25.2	1492	94.1	3163	9.4

Table S3. Optimized structure of the transition state TS2 from singlet carbene to beta-lactam and B3LYP/6-31+G(d) level of theory. Transition state were obtained from QST2 method and were confirmed with IRC calculation.

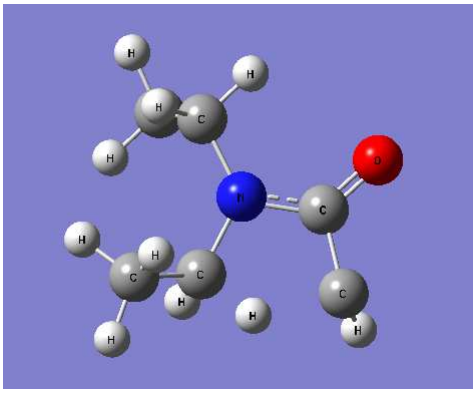

Energy = -365.11974372

C	1.350821000	-0.257373000	-0.058775000
C	2.031504000	0.980121000	0.319077000
H	2.350820000	0.956168000	1.374446000
O	1.997763000	-1.271881000	-0.332535000
N	-0.004020000	-0.063473000	-0.137501000
C	-0.323678000	1.233151000	0.419142000
H	-0.589367000	1.191388000	1.483449000
H	0.709776000	1.790311000	0.364752000
C	-1.293673000	2.085304000	-0.387299000
H	-2.292871000	1.632454000	-0.392499000
H	-1.384211000	3.081929000	0.057313000
H	-0.954569000	2.190234000	-1.422906000
C	-0.961281000	-1.073745000	-0.563091000
H	-0.366682000	-1.851589000	-1.051950000
H	-1.626392000	-0.643812000	-1.323300000
C	-1.776927000	-1.672981000	0.588134000
H	-2.381291000	-0.913379000	1.099280000
H	-2.461541000	-2.438589000	0.204212000
H	-1.118243000	-2.142614000	1.326859000

Frequency (cm^{-1})	IR intensity (km/mol)	Frequency (cm^{-1})	IR intensity (km/mol)	Frequency (cm^{-1})	IR intensity (km/mol)
-303	40.0	955	20.8	1503	16.1
51	0.4	978	3.5	1512	9.0
98	3.6	996	50.1	1516	6.9
117	2.7	1055	1.5	1517	2.3
190	1.8	1096	8.2	1526	5.2
210	0.1	1107	1.5	1710	378.4
258	4.4	1135	5.2	2154	193.0
300	4.4	1194	1.1	3045	16.6
327	6.0	1261	8.2	3046	21.6
434	7.0	1342	41.7	3053	2.1
498	8.4	1361	42.0	3053	47.6
592	29.9	1395	34.8	3056	31.1
614	17.0	1403	8.2	3101	15.1
722	1.3	1424	2.3	3116	18.8
763	5.0	1431	18.2	3118	21.1
791	3.2	1434	10.6	3127	21.4
882	25.2	1492	94.1	3163	9.4

References:
(1) Becke, A. D. *J. Chem. Phys.* **1993**, *98*, 5648-5652.
(2) Becke, A. D. *J. Chem. Phys.* **1992**, *96*, 2155-2160.
(3) Becke, A. D. *J. Chem. Phys.* **1992**, *97*, 9173-9177.
(4) Lee, C.; Yang, W.; Parr, R. G. *Phys. Rev. B* **1988**, *37*, 785-789.
(5) Frisch, M. J.; Gaussian 03, Revision C.02 ed.; Gaussian, Inc.: Wallingford CT, 2004.
(6) Mennucci, B.; Tomasi, J. *J. Chem. Phys.* **1997**, *106*, 5151-5158.